

HEAT TRANSFER ENHANCEMENT OF FALLING FILM EVAPORATION ON A HORIZONTAL TUBE BUNDLE

Mostafa M. Awad * and El-Sayed R. Negeed **

* Mansoura University, Faculty of Engineering, Mechanical Power Dept., Egypt
E-mail: mostawad100@yahoo.com

** Atomic Energy Authority, Nuclear Research Center, Reactors Dept., Cairo, Egypt
E-mail: s.negeed@gmail.com

ABSTRACT

The enhancement of the evaporation heat transfer coefficient is important for the design and operation of horizontal tube spray film evaporators. The water spray on a horizontal tube bundle is numerically studied in steady state conditions. The objective of the present work is to numerically study the effect of the tube configuration and the operating conditions on the evaporation heat transfer coefficient. In addition, the enhancement of the evaporation rate ratio by constructing a water collector around the bottom-heated tube is also numerically studied. In order to evaluate the evaporation rate ratio and the heat transfer coefficient of the falling liquid film on the horizontal tube bundle, the non-dimensional governing equations of the mass, momentum and energy of the created liquid film around the hot tube surface are solved numerically using the finite difference method. The results show that the evaporation rate ratio is mainly increased by increasing both the surface temperature and the tube's outer diameter. The evaporation rate ratio enhances by decreasing the chamber pressure and inlet liquid subcooling. The falling distance has little influence on the evaporation rate ratio. Moreover, constructing a water collector around the bottom-heated tube enhances the evaporation rate ratio. The increase in the evaporation rate ratio increases by higher heat flux and also by larger the gap between the collector and the tube surface.

Keywords: Desalination; horizontal tube evaporator; tube bundle, heat transfer enhancement; liquid film evaporation; liquid collector.

NOMENCLATURE

A_o	Tube outer surface area, m^2
C_p	Specific heat at constant pressure, $J/kg.K$
D	Droplet diameter after falling distance, m
d	Differentiation sign.
D_1	Droplet initial diameter, m
d_{ot}	Tube outer diameter, m
g	Acceleration due to gravity, m^2/s

h'	Average heat transfer coefficient, W/m^2K
h_{fg}	Latent heat for vaporization, J/kg
L	Tube length, m
M	Molecular weight.
m'_w	Sprayed mass flow rate, kg/s
m'_v	Evaporation rate, kg/s
N_C	Number of columns in the bundle
p	Pressure, N/m^2
p_{spr}	Spray pressure, N/m^2
q	Heat flux, W/m^2
Q_t	Transmitted heat, W
r	radius, m
S	Size of the gap between the liquid collector and the tube surface, m
t_1	Sprayed water inlet temperature, K
t_2	Droplet temperature after the falling distance, K
t_s	Temperature of the tube outer surface, K
t_v	Evaporation temperature, K
V	Volume, m^3
v	Velocity, m/s
v_1	Droplet initial velocity, m/s
v_2	Droplet velocity after the falling distance, m/s
ZZ	Droplet falling distance (vertical distance from the nozzle to the tube surface), m

Greek Letters

Γ	Sprayed mass flow rate per one side of the hot tube surface, $kg/s.m$
$\Delta t_{sup.}$	Superheating (the difference between the hot surface temperature and the formed vapor saturation temperature), K
$\Delta t_{sub.}$	Subcooling (the difference between the formed vapor saturation temperature and the sprayed water initial temperature), K
δ	Liquid layer thickness, m
ρ	Density, kg/m^3
σ	Surface tension, N/m
τ	Time, s
μ	Dynamic viscosity, $N.s/m^2$

Subscripts

f	Liquid film
1	Initial value
2	At the falling distance zz
V	Vapor
w	Water

Abbreviations

η_{ev} Evaporation rate ratio, the ratio between the evaporation rate and the initial sprayed mass flow rate.

Dimensionless numbers

Nu Nusselt number, $= h d_{ot} / k_f$

Re_f Falling Reynolds number, $= 4 \Gamma / \mu_w$

1. INTRODUCTION

As the price of fossil fuel highly increases worldwide, the economics of the thermal devices and unit shall be improved and enhanced so as to save the energy cost in the energy conversation and energy conversion equipments. The expected results of the promising current investigation will augment the heat transfer modes, surfaces, coefficients in the spray- falling liquid film evaporators and increases its effectiveness. Therefore, Heat transfer through falling film or spray film evaporation shall serve the heat exchange devices which are used in desalination and ocean thermal energy conversion (OTEC) systems. The horizontal tube evaporators basically consist of a bundle of horizontal tubes connected by headers at each end, as in the conventional shell and tube heat exchangers. The shell side liquid is introduced through spray nozzles to the top of the bundle and subsequently drains on top of the lower tube banks where liquid films flow and evaporate on the outside tube surfaces. The maximum spread of a droplet upon impact on a hot surface, depends mainly on the liquid viscosity and liquid-surface contact angle, while, the tendency of a droplet to deposit or rebound is determined primary by the droplet impinging speed and hot surface temperature. This will create a liquid film on the evaporator tube surface that has a direct effect on the heat transfer coefficient and on the evaporation rate ratio. The evaporator effectiveness will depend on how the liquid film falls from one tube to another. As the flow rate varies, three basic flow patterns may be observed: discrete droplets, jets or continuous sheet, Wei and Jacobi ^[1]. At a very low flow rate, the liquid departs from the bottom of the tube in droplet mode. A gradual increase in the flow rate can cause a transition from droplets to jets, where at higher flow rates a transition will be from jets to a liquid sheet. Hu and Jacobi ^[2] provided the first generalized flow-pattern maps for predicting falling-film mode. The map includes the different modes. It should be noted that in the present study the liquid sheet falling between horizontal tubes mode is considered. The spray cooling heat exchanger was studied numerically and experimentally by Negeed ^[3]. He studied the effect of the operating conditions of the heat transfer effectiveness for the horizontal tube bundle and the tubes were arranged as inline. Also, experimental study of falling film evaporation heat transfer outside horizontal tubes was studied by Yang and Shen ^[4]. They studied experimentally the effect of the flow density, evaporation temperatures, distributor height, temperature difference between wall and saturation water, and mass concentration of the seawater on the heat transfer coefficient. The principal advantages

of spray film evaporators are high heat transfer rates at small temperature differences. The spray film evaporation process can provide a better heat transfer performance than pool boiling, particularly at low heat fluxes; on the other hand spray cooling can not impact directly on the bottom surfaces of the horizontal tubes. Therefore, the lower surfaces of the tubes receive relatively less coolant and are hence more susceptible to dry-out phenomenon to occur on the bottom surfaces, Chang and Chiou^[5]. This problem is particularly accurate for the tubes located in the bottom rows of the bundle. Under low surface heat fluxes, the sprayed liquid is sufficient for cooling all the tubes. However, when the surface heat flux is high, the thin liquid film may evaporate completely at the lower surface of the tube and the dry-out phenomenon occurs. Clearly, the heat transfer coefficient falls significantly when the films dries out. This study constructs liquid collector beneath each heated tube to collect the liquid which bounces from the heated tube surface or falls along its circumference. The liquid collector not only impedes the dry-out phenomenon, but also, guides the overflow liquid directly to the upper surfaces of the tubes in the lower row.

The main objective of this study is to investigate numerically the effect of the arrangement of the tubes and the operating conditions on the evaporation rate ratio by spraying water upon the hot surfaces and the tubes are arranged as staggered. Therefore, the present work studies the effect of the inlet sprayed flow rate per unit area of the hot surface, evaporation pressure, hot tube surface temperature, falling distance and inlet spray subcooling on the evaporation rate ratio. In addition, the effect of constructing the liquid collector around the bottom of the tube surface bundle on the evaporation rate ratio is also studied.

The tube bundle contains eight stainless steel tubes, arranged in staggered (triangular) form in three rows. The first row contains three tubes, the second row contains two tubes and the third row contains three tubes. The pitch to tube diameter ratio is only 1.46 (an average value for staggered tubes).

Figures (1.a) and (1.b) show Liquid film distribution in triangular pitch tube bundle for non constructing liquid collectors and for constructing liquid collectors around the tube bundle respectively. In this study, the liquid collectors as shown in Fig. (1.b) are made from copper sheet and are clipped to the underside of each tube. The collectors are slightly larger than the tubes diameters and are designed to collect both the liquid droplets which bounce back from the tube surface and non-evaporated liquid which falls along the tube circumference. The gap between the tube and the liquid collector is varied from 2 to 4 mm.

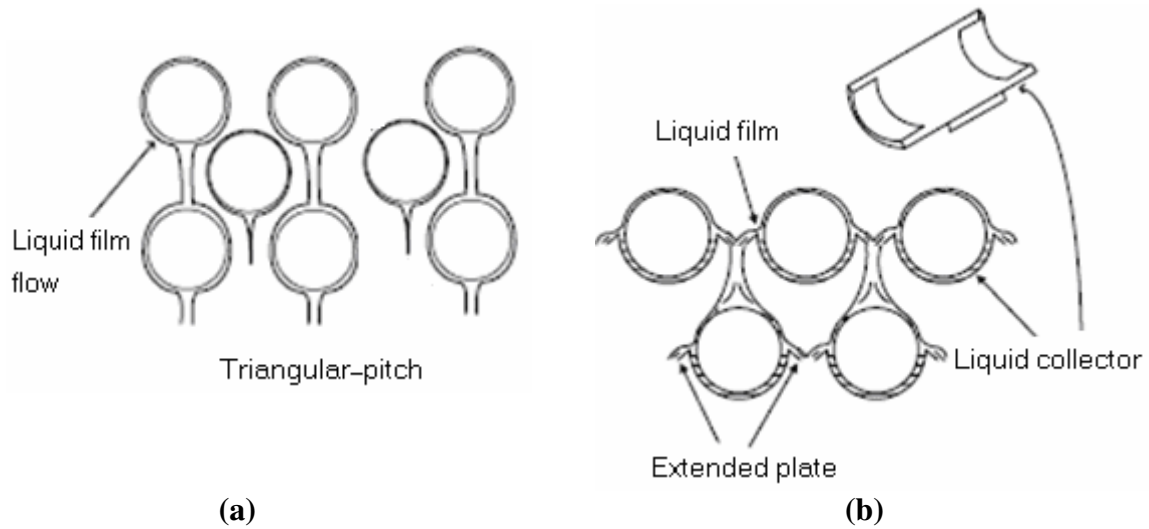


Fig. (1) Liquid film distribution around the tube bundle in cases of;
a) without liquid collectors b) with liquid collectors

2. MATHEMATICAL MODEL

Change in Droplet Velocity, Size and its Temperature for the Region from the Nozzle up to the Hot Tube Surface

The droplet is exposed to many forces in the region between the nozzle and the tube surface:

The gravitational force which is:
$$F_1 = \frac{g \pi D^3 \rho_w}{6} \quad (1)$$

The buoyancy force which is:
$$F_2 = \frac{\pi g D^3 \rho_v}{6} \quad (2)$$

The drag force which is:
$$F_3 = \frac{C_D \pi D^2 \rho_v (v_w - v_v)^2}{8} \quad (3)$$

The coefficient of drag force (C_D) can be calculated as a function of Reynolds number as a function of the physical properties of the droplet, Re_d , from the following relation (Tanaka drag law) by Linn et al.^[6].

$$\begin{aligned} C_D &= \frac{24}{Re_d} && \text{for } Re_d < 2 \\ &= \frac{10}{Re_d} && \text{for } 2 < Re_d \leq 500 \\ &= 0.44 && \text{for } 500 \leq Re_d < 10^5 \end{aligned} \quad (4)$$

The momentum equation of the water droplet is given as:

$$m \frac{dv}{d\tau} + v \frac{dm}{d\tau} = \sum F \quad (5)$$

Where $\sum F$ is the summation of the effective forces on the droplet, i.e.

$$\Sigma F = F_1 - F_2 - F_3 \quad (6)$$

So, the momentum equation of the water droplet leaving the nozzle is written as:

$$\frac{\pi D^3 \rho_w dv_w}{6 d\tau} + \frac{(v_w - v_v) d(\frac{\pi}{6} D^3 \rho_w)}{d\tau} = \frac{g \pi D^3 \rho_w}{6} - \frac{\pi g D^3 \rho_v}{6} - \frac{C_D \pi D^2 \rho_v (v_w - v_v)^2}{8} \quad (7)$$

The vapor velocity can be negligible compared with the sprayed water velocity, Ibrahim⁽⁷⁾. i.e. $v_v \approx 0.0$ then, equation (7) can be rewritten as:

$$\frac{dv_w}{d\tau} = \frac{(\rho_w - \rho_v)g}{\rho_w} - \frac{3C_D \rho_v v_w^2}{4\rho_w D} - \frac{v_w}{D^3} \frac{dD^3}{d\tau} \quad (8)$$

If the term $\frac{dD^3}{d\tau} = 3D^2 \frac{dD}{d\tau}$, then equation (8) is reduced to

$$\frac{dv_w}{d\tau} = \frac{(\rho_w - \rho_v)g}{\rho_w} - \frac{3C_D \rho_v v_w^2}{4\rho_w D} - \frac{3v_w}{D} \frac{dD}{d\tau} \quad (9)$$

The change rate of droplet diameter ($\frac{dD}{d\tau}$) can be obtained from the following equation, Lekic and Ford^[8]:

$$\frac{dD}{d\tau} = \frac{2\pi^2 \alpha \varepsilon}{D_l} \frac{e^{-\pi^2 f_o}}{(1 - e^{-\pi^2 f_o})^{1/2}} \quad (10)$$

where

$$\varepsilon = (1 + cp_w \left(\frac{t_v - t_1}{h_{fg}}\right)^{1/3}) - 1 \quad (11)$$

$$\alpha = \frac{k_w}{\rho_w cp_w} \quad (12)$$

$$f_o = \frac{4(\tau_2 - \tau_1)\alpha}{D_1^2} \quad (13)$$

The change of droplet diameter during condensation can be solved from the following equation, Lekic and Ford [8]:

$$D = D_1[1 + \varepsilon(1 - e^{-\pi^2 f_o})^{\frac{1}{2}}] \quad (14)$$

By solving the equations (9), (10) and (14), then the droplet velocity (v) can be estimated in terms of droplet initial diameter (D_1), droplet initial velocity (v_1), droplet initial temperature (t_1) and saturation temperature (t_v).

During the contact of water droplets with the vapor, heat is transferred between the two phases and the droplet temperature (t_2) at distance ZZ from the nozzle can be calculated from the following equation, Lim et al. [9]:

$$t_2 = \frac{1}{cp_w} \left[\frac{D_1^3 (cp_w t_1 - h_v)}{D^3} + h_v \right] \quad (15)$$

where, the enthalpy of vapor (h_v) is a function of the evaporation pressure.

The Region around the Heated Tube Surface

For without the liquid collectors around the heated tube surface

As shown in Fig. (2), due to the spraying of water, a thin film is formed around the horizontal tube. The tube wall temperature is assumed to be constant and denoted as t_s and also the saturation temperature of the falling water t_v corresponding to the surrounding pressure. Also, in this evaluation the coordinates (r, θ) are used. The average water film tangential velocity and the film thickness are denoted as v' and δ respectively. The heat transfer occurs as a result of falling film evaporation.

Governing Equations

To simplify the describing equations of heat transfer process through the thin film some assumptions were made as:

- Conduction heat transfer takes place in radial direction (r -direction) while heat transfer by convection is assumed in the tangential direction (θ -direction).
- The flow around the tube is assumed to be one directional flow in tangential direction.
- The wall temperature is constant and uniform.
- The entire tube surface is covered with liquid film; (there is perfect wetting).

- The film flow is laminar, steady and ideal.
- The film thickness is small compared to the tube diameter.
- There is no nucleate boiling within the film.
- Evaporation occurs on the liquid- vapor interface where the temperature is at saturation.
- The surface tension effect is negligible.

According to the foregoing assumptions the continuity, momentum and energy equations in the cylindrical coordinates are simplified to the following forms:

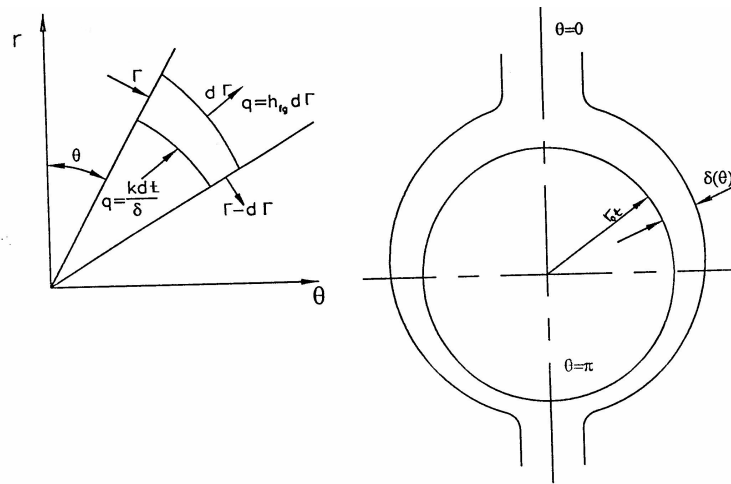


Fig. (2). Heat balance of a general element

$$\frac{1}{r} \frac{\partial ru}{\partial r} = \frac{\partial w}{\partial z} - \frac{1}{r} \frac{\partial v}{\partial \theta} \tag{16}$$

$$\frac{v \rho}{r} \frac{\partial v}{\partial \theta} = g(\rho_w - \rho_v) \sin(\theta) + \mu_w \left[\frac{1}{r} \frac{\partial}{\partial r} \left(r \frac{\partial v}{\partial \theta} \right) + \frac{1}{r^2} \frac{\partial^2 v}{\partial \theta^2} \right] \tag{17}$$

$$\rho c_p \frac{v}{r} \frac{\partial t}{\partial \theta} = k_f \left[\frac{1}{r} \frac{\partial}{\partial r} \left(r \frac{\partial t}{\partial r} \right) + \frac{1}{r^2} \frac{\partial^2 t}{\partial \theta^2} \right] \tag{18}$$

The boundary conditions are:

$$\begin{aligned} \text{at } r = r_{ot} \quad & v = 0, \quad t = t_s \\ \text{at } r = r_{ot} + \delta(\theta) \quad & \frac{\partial v}{\partial r} = 0, \quad t = t_v \end{aligned} \tag{19}$$

Where, $\delta(\theta)$ is the film thickness around the tube at the angular position (θ) .

Estimation of the formed film thickness and the evaporation rate

In order to estimate the film thickness, as a first approximation used to obtain the first solution of the governing equations, the temperature profile is assumed to be linear. Also, the heat transfer from the hot surface to the sprayed liquid is due to conduction only. Thus, the overall energy balance of the element can be made. This is carried out by assuming that heat is conducted across the film in the radial direction and evaporation takes place at the free surface. Also, the viscous force in tangential direction is taken in account, while that in radial direction is negligible. Furthermore, the inertia terms in radial and axial directions are neglected and the derivative of velocity that respect to θ direction can be neglected.

Thus the mean velocity across the film thickness can be presented as:

$$v' = \frac{g(\rho_w - \rho_v)\sin(\theta)}{4\mu_w} r_{ot} \delta \sin(\theta) \quad (20)$$

The mass flow rate at any position can be determined by applying the conservation law of mass as:

$$\Gamma = \rho_w v' \delta(\theta) \quad (21)$$

where, v' is the average film velocity and Γ is the mass flow rate per unit length per one side at any position of tube.

From equations (20) and (21), the film thickness as a function of θ can be given as:

$$\delta(\theta) = \left[\frac{4\mu_w \Gamma}{r_{ot} g \rho_w (\rho_w - \rho_v) \sin(\theta)} \right]^2 \quad (22)$$

Assuming approximate value of $\delta(\theta)$ to equation (22) as a first guess then, equations (16) to (18) are solved numerically using finite difference technique. Hence, the differential equations are approximated by a set of simultaneous linear equations. The Gauss-Seidel iterative method is applied to solve these equations. The numerical solution of the equations is carried out in successive manner, i.e. the obtained solution of the equations at certain cross section (certain value of radius r) is dependent upon the previously obtained value of the cross section (preceding the radius r) and so on. In which the velocity and temperature distributions throughout the flow film can be obtained. Therefore, the value of the local and average heat transfer coefficient can be calculated. The overall heat balance of this element can be presented as:

$$-d\Gamma(h_{fg}) = k_f \left(\frac{t_s - t_v}{\delta} \right) r d\theta \quad (23)$$

Accordingly, $\Gamma_o(\theta=0.0)$ is the mass flow rate of the falling film per unit length of the tube.

Equation (22) can be rewritten as:

$$\delta_n(\theta) = \left[\frac{-k(t_s - t_v)r d\theta}{h_{fg} d\Gamma} \right]^2 \quad (24)$$

where, $\delta_n(\theta)$ is noted as the improved value for the film thickness. If the result of the comparison between the improved value of the film thickness $\delta_n(\theta)$ and the approximate value of $\delta(\theta)$ is not satisfactory, the foregoing steps of the solution are repeated till; the error is within allowable prescribed value.

The local heat transfer coefficient and local Nusselt number can be determined according to the following equations:

$$h_o = \frac{q_w}{t_s - t_v} = \left(\frac{-k_f}{t_s - t_v} \right) \left[\frac{\partial t}{\partial r} \right]_{r=r_{ot}} \quad (25)$$

$$Nu = \frac{h_o d_{ot}}{k_f} \quad (26)$$

and the average heat transfer coefficient (h') is given as:

$$h' = \frac{1}{\pi} \int_0^\pi h_o d\theta \quad (27)$$

The evaporation rate can be calculated as:

$$m'_{ev} = \frac{h' A_{ot} (t_s - t_v)}{cp_1(t_v - t_1) + h_{fg}} \quad (28)$$

Where,

$$A_{ot} = \pi d_{ot} L \quad (29)$$

For constructing the liquid collectors around the bottom heated tube surface

In the case of constructing the liquid collectors around the bottom heated tube surface, the heat transfer at the upper surface area of each tube (i.e. the area which is not

covered by the liquid collector) occurs as a result of falling film evaporation. The remaining surface area of the heat transfer is one of narrow gap boiling. The heat transfer in the case of constructing the liquid collectors are the summation of the heat transfer due to falling film evaporation on the upper tube surface, see the above section, and the heat transfer due to the boiling in the narrow gap generated by current tube/liquid collector configuration.

Boiling in the gap space is mainly characterized by the deformation of the bubbles. The bubble deformation can be characterized by the ratio of the gap size and the nominal bubble departure diameter, which is generally known as the Bond number (B_o), Chang and Chiou^[5]:

$$B_o = \frac{S}{(\sigma / g (\rho_l - \rho_v))^{1/2}} \quad (30)$$

Where S is the gap size and $(\frac{\sigma}{g (\rho_l - \rho_v)^{1/2}})$ is the bubble size. Chang and Chiou⁽⁵⁾

reported that when the Bond number excess one, the heat transfer performance of narrow gap boiling is comparable to that of pool boiling. The gap size used in the present study is ranged from 2.0 to 4.0 mm and the corresponding Bond number excess one. The boiling heat transfer coefficient in this gap can be calculated from the following correlation, Cooper^[10]:

$$h_b = 90(q_b)^{0.67} M^{-0.5} p_{cr}^c (-\log_{10} P_r)^{-0.55} \quad (31)$$

Where

$$q_b = h_b (t_s - t_v) \quad (32)$$

$$c = 0.12 - 0.2 \log_{10} R_p \quad (33)$$

R_p indicates the mean surface roughness and is measured in units of μm .

$$P_r = \frac{p_v}{p_{cr}} \quad (34)$$

p_v is the saturation pressure and p_{cr} is the critical pressure

The evaporation rate due to the pool boiling in the gap between the liquid collector and the surface tube can be calculated as:

$$m'_b = \frac{h_b A_{ot} (t_s - t_v)}{cp_1(t_v - t_1) + h_{fg}} \quad (35)$$

Calculation of the evaporation rate ratio of the tube bundle

The total amount of the evaporation rate (m'_t) is the summation of the evaporation rate due to the falling film evaporation on the upper tube surface (m'_{ev}) that calculated from equation (28) and the evaporation rate due to the pool boiling in the gap between the liquid collector (m'_b) that calculated from equation (35) therefore,

$$m'_t = m'_{ev} + m'_b \quad (36)$$

From which, the amount of the falling mass flow rate of the second lower tube in the next row ($m'_{ws,2}$), can be calculated as:

$$m'_{ws,2} = m'_{ws,1} - m'_t \quad (37)$$

Then, the liquid film thickness, average heat transfer coefficient and evaporation rate for the second row can be evaluated. Also, the mass flow rate of the third row can be calculated by the same previous procedure. And so on for the next lower row in the bundle.

The evaporation rate ratio for the bundle can be calculated from the following equation:

$$\eta_{ev} = \frac{1}{m'_{ws,1}} \sum_{i=1}^{i=n_t} m'_{t,i} \quad (38)$$

Where, n_t is the number of rows of the bundle, and $m'_{ws,1}$ is the mass flow rate of the first vertical row in the bundle.

3. RESULTS AND DISCUSSIONS

Effect of the falling distance and surface temperature difference on the evaporation rate ratio

Figure (3) shows that, the droplet falling distance ratio (zz/zz_{max}) has a little effect on the evaporation rate ratio. And, as the surface temperature difference ($t_s - t_v$) increases, the evaporation rate ratio (η_{ev}) increases. This is because by increasing the surface temperature difference, the heat transfer from the hot surface to the liquid film increases therefore, the amount of the evaporated rate ratio will increase. Also, by constructing water collector around the bottom heated tube, the evaporation rate ratio will increase. The increase in the evaporation rate ratio increases with higher surface temperature difference. Also, by constructing water collector around the bottom heated tube the evaporation rate ratio will increase. Moreover, the evaporation rate ratio is

relatively proportional to the gap between the liquid collector and the tube diameter. This is because the pool boiling in the space between the hot surface and the liquid collector increases with the increase in the gap size.

Effect of the evaporation pressure and surface temperature difference on the evaporation rate ratio

Figure (4) shows that, the evaporation rate ratio increases with decreasing the evaporation pressure. That is due to the temperature difference between the hot surface and the evaporation temperature increases by decreasing the evaporation pressure; hence, the amount of the heat transfer from the hot surface to the formed liquid film will increase. Moreover, by constructing water collector around the bottom heated tube the evaporation rate ratio will increase. The increase in the evaporation rate ratio increases by lowering the applied evaporation pressure.. Also, the evaporation rate ratio is relatively proportional to the gap between the liquid collector and the tube diameter. This is because the pool boiling in the space between the hot surface and the liquid collector increases by increasing the gap size.

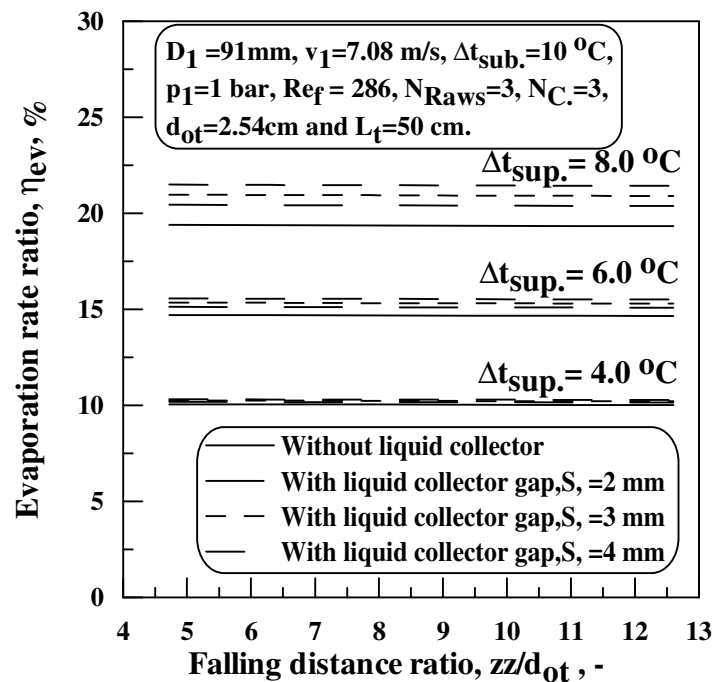


Fig. (3). Effect of falling distance and surface temperature difference on evaporation rate ratio for non constructing liquid collectors and for constructing liquid collectors

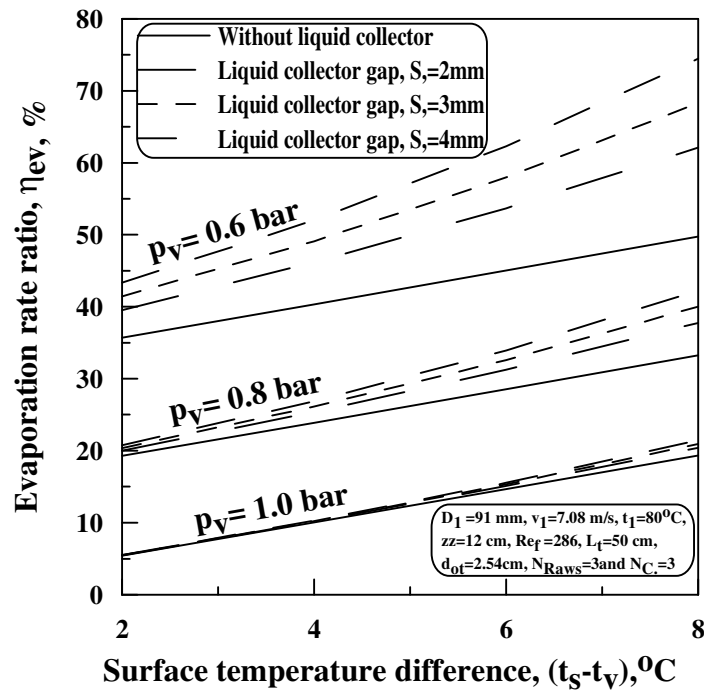


Fig. (4). Effect of the surface temperature difference and the evaporation pressure on evaporation rate ratio for non constructing liquid collectors and for constructing liquid collectors

Effect of Initial Sprayed Subcooling and Surface Temperature Difference on Nusselt number

Figure 5 shows that as the surface temperature difference ($t_s - t_v$) increases, Nusselt number (Nu) increases. Also, Nusselt number increases with a decrease in the initial sprayed subcooling. That is due to the decrease of the water layer thickness, which tends to reduce the heat transfer from the hot tube surface to the sprayed water. Moreover, by constructing the water collector around the bottom-heated tube, Nusselt number will increase. The increase in Nusselt number increases with higher surface temperature difference.

Effect of Initial Sprayed Mass Flow Rate and Surface Temperature Difference on the Evaporation Rate Ratio

Figure (6) shows that, the evaporation rate ratio increases with decreasing the initial sprayed mass flow rate per unit length per one side of the tube (Γ). That is because, the water layer thickness ratio (δ/d_{ot}), equation (32) increases by increasing the initial sprayed mass flow rate per unit length per one side of the tube and it tends to reduce heat transfer from the hot tube surface to the sprayed liquid. Moreover, by constructing water collector around the bottom heated tube the evaporation rate ratio will increase. The increase in the evaporation rate ratio increases by lowering the initial sprayed

mass flow rate per unit length per side of the tube. Also, the evaporation rate ratio is relatively proportional to the gap between the liquid collector and the tube diameter.

Effect of Tube Outer Diameter and Surface Temperature Difference on the Evaporation rate ratio

Figure (7) shows that, the evaporation rate ratio is relatively proportional to the tube outer diameter. This is because the heat transfer from the hot surface to the liquid film increases by increasing the tube outer diameter. Moreover, the formed liquid layer decreases by increasing the tube outer diameter. This is because the sprayed mass flow rate per unit length per one side of the tube (Γ) increases by decreasing the tube outer diameter. Also, by constructing water collector around the bottom heated tube the evaporation rate ratio will increase. The increase in the evaporation rate ratio increases with larger tube's outer diameter. Also, the evaporation rate ratio is relatively proportional to the gap between the liquid collector and the tube diameter. This is because the pool boiling in the space between the hot surface and the liquid collector increases with the increase in the gap size.

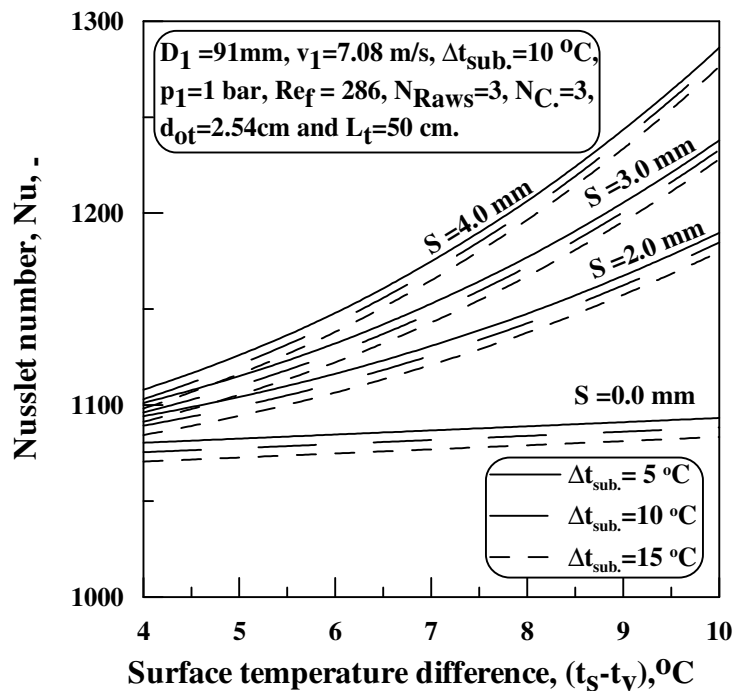


Fig. (5). Effect of the surface temperature difference and the initial sprayed subcooling on Nusslet number for non constructing liquid collectors and for constructing liquid collectors

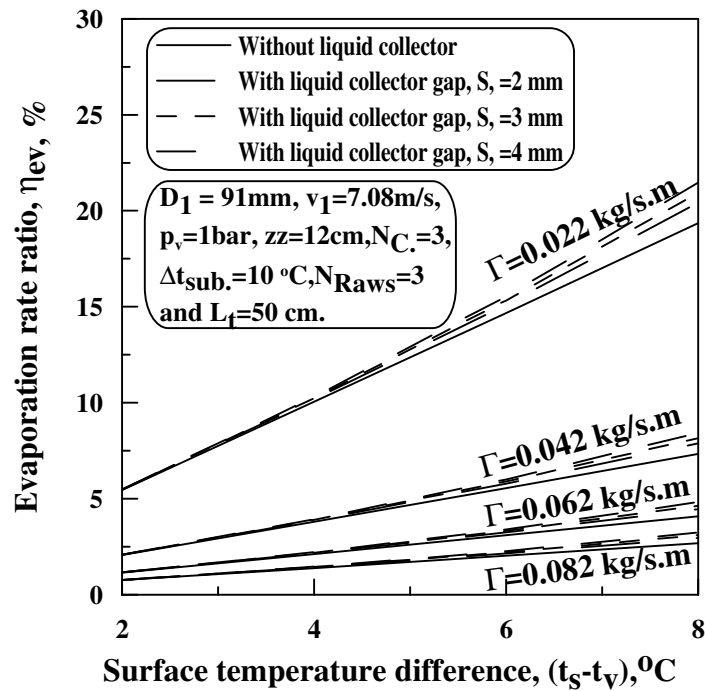


Fig. (6). Effect of the surface temperature difference and the initial sprayed flow rate on the evaporation rate ratio for non constructing liquid collectors and for constructing liquid collectors

Effect of the Gap between the Liquid Collector and the Hot Tube diameter on the Evaporation rate ratio for Different Surface Temperature

Figure (8) shows that, the evaporation rate ratio is relatively proportional to the gap between the liquid collector and the tube diameter. This is because the pool boiling in the space between the hot surface and the liquid collector increases by increasing the gap size. Also, by constructing water collector around the bottom heated tube the evaporation rate ratio will increase.

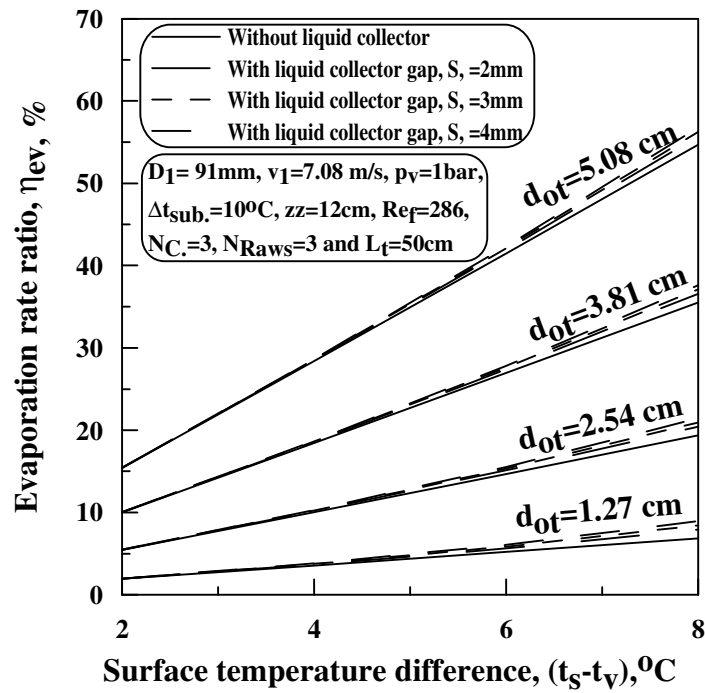


Fig. (7). Effect of the surface temperature difference and the hot tube outer diameter on the evaporation rate ratio for non constructing liquid collectors and for constructing liquid collectors

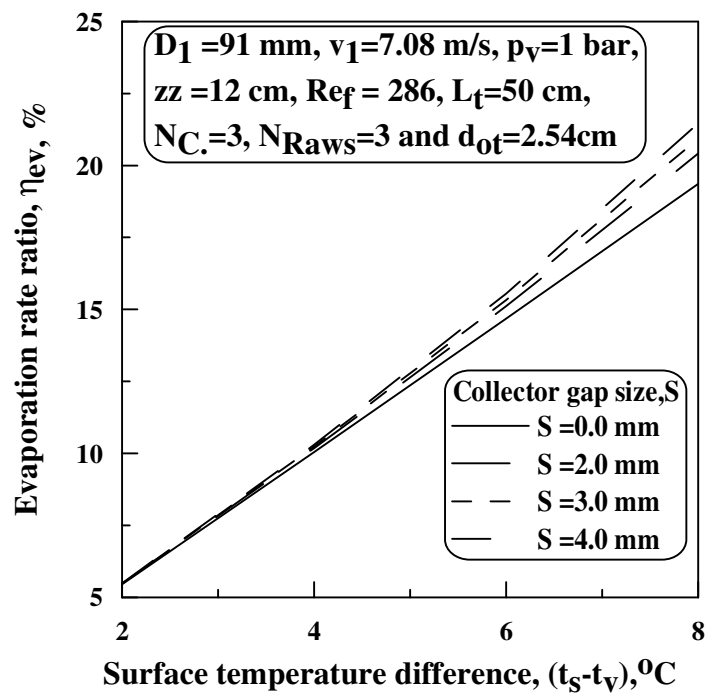


Fig. (8). Change of evaporation rate ratio against the surface temperature difference for different values of the gab between the liquid collector and the tube diameter

4. CONCLUSIONS

From this study, the following conclusions can be drawn: The evaporation rate ratio is mainly increased by increasing the surface superheating and by increasing the tube outer diameter. Decreasing the chamber pressure, inlet liquid subcooling and sprayed mass flow rate result in increase of the evaporation rate ratio. Also, by constructing water collector around the bottom heated tube, the evaporation rate ratio will increase. The increase in the evaporation rate ratio increases by higher surface heat flux. In addition, the evaporation rate ratio increases by increasing the gap between the collector tube and the tube surface from about 2.0 to 4.0 mm.

REFERENCES

1. Y. H. Wei and A. M. Jacobi, "Vapor-shear, geometric and bundle- depth effects on the inter tube falling- film modes, the inter tube falling film: Part 1, flow characteristics, mode transitions and hysteresis", 1st International Conference on Heat Transfer, Fluid Mechanics, and Thermodynamics, 8-10 April 2002, Kruger Park, South Africa.
2. X. Hu and A. M. Jacobi, "Vapor-shear, geometric and bundle-depth effects on the inter tube falling-film modes", *The Inter tube Falling Film: Part 1, Flow Characteristics, Mode Transitions and Hysteresis*, Journal of Heat Transfer, Vol. 118, 1996, pp. 616-625.
3. T. B. Chang and J. S. Chiou, "Spray evaporation heat transfer of R-141 b on a horizontal tube bundle", *International Journal of Heat and Mass Transfer*, Vol. 42, 1999, pp. 1467-1478.
4. El-Sayed R. Negeed, "Spray Cooling Heat Exchangers", Ph. D. Thesis, mechanical power engineering, faculty of engineering, Cairo university, 2004.
5. Luopeng Yang and Shengqiang Shen, "Experimental study of falling film evaporation heat transfer outside horizontal tubes", *Desalination* Vol. 220, 2008, pp. 654-660.
6. Jeremy D. M. Linn, Stephen, J. Maskell and Mike A. Patrick, "A note on heat and mass transfer to a spray droplet", *Nuclear Technology*, Vol. 81, Apr. 1988, pp. 122-125.
7. N. A. Ibrahim, "Effectiveness of containment depressurization spray system in nuclear reactors", Ph. D. Thesis, Zagazig university, Egypt, 1989.
8. Lekic. A. and J. D. Ford, "Direct contact concentration of vapor on a spray of subcooled liquid droplets", *Int. J. Heat Mass Transfer*, Vol. 23, 1980, pp. 1531-1537.
9. S. Lim, R. S. Tankin and M. C. Yuen, "Condensation measurements of horizontal steam/ water flow", *Journal of Heat Transfer*, Vol. 106, May 1984, pp. 425-482.
10. M. G. Cooper, "Saturation nucleate, pool boiling-ma simple correlation", *International Chemical Engineering Symp.*, Vol.86, 1984, pp. 785-792.